

Composites based on ZrO_2 - $CaAl_4O_7$ using conventional sintering and spark plasma sintering (SPS)

Y.L. Bruni^a, G. Suarez^a, Y. Sakka^b, L.B. Garrido^a and E.F. Aglietti^{a*}

^aCentro de Tecnología de Recursos Minerales y Cerámica (CETMIC): (CIC-CONICET-CCT La Plata), Camino Centenario y 506, C.C.49 (B1897ZCA) M.B.Gonnet, Buenos Aires, Argentina

^bFine Particle Processing Group, Nano Ceramics Center, National Institute for Materials Science (NIMS), 1-2-1, Sengen, Tsukuba, Ibaraki 305-0047, Japan

Composites based on ZrO_2 stabilized with CaO and $CaAl_4O_7$ were sintered via two different techniques: Conventional Sintering route and Spark Plasma Sintering (SPS) between 1200 and 1400 °C. The effectiveness of sintering technique applied on the stabilization degree of ZrO_2 (conversion to c- ZrO_2 , $Ca_{0.15}Zr_{0.85}O_{1.85}$), microstructure, densification and Vickers hardness of the composites was evaluated. The SPS represented a remarkable advance in the c- ZrO_2 formation and also resulted in a high densification of the composites (inclusive at 1200 °C) which attained relative densities higher than 0.95. The advantage of SPS technique was mainly evidenced by the high densification of composites with high $CaAl_4O_7$ content. Therefore, the composites sintered by SPS exhibited higher hardness (10 GPa) compared to that of composites produced via conventional sintering (6 GPa).

Key words: ZrO_2 composites, Ca-stabilized zirconia, Spark plasma sintering, Calcium dialuminate.

Introduction

Spark Plasma Sintering SPS currently represents a technological advance in the ceramic powders consolidation because it allows an optimum sintering at lower temperatures and shorter times compared with other conventional sintering techniques [1-3]. This technique basically consists of the simultaneous application on the powder to be sintered of a high voltage current pulse and uniaxial pressure, those combined effects lead to a substantial improvement on the densification processes and therefore, in a progress of mechanical properties. SPS is fundamentally different from conventionally heating, in which heating occurs through surface by conduction, radiation, and convection. In Spark Plasma Sintering the heat is first transferred onto material surface and then moves inward.

Composites based on ZrO_2 stabilized with CaO and calcium dialuminate ($CaAl_4O_7$) can be developed from mixtures of pure zirconia (m- ZrO_2) and high alumina cement containing CaO by a reaction sintering process at 1300-1500 °C [4]. The green composites were shaped by uniaxial pressing and subsequently sintered via the conventional pressureless method at the mentioned range of sintering temperatures. One of the phases present in these composites was the calcium stabilized zirconia

(CSZ) that has specific applications in various technological fields, mainly for metal and electronics industries [5-6]. Conventional methods to obtain CSZ include: microwave sintering of ZrO_2 with calcium compounds as $CaCO_3$ or dolomite [7], sol-gel method by using a polymer technique [8], high energy milling of ZrO_2 nanoparticles and dolomite [9] and chemical precipitation of ZrO_2 -Hydroxyapatite powders [10]. Currently, sintering of CSZ by SPS has not been reported in the literature. However, sintering of yttria stabilized zirconia ceramics (3Y- ZrO_2 , 8Y- ZrO_2) by SPS were previously investigated [11-13].

The other phase present in the composites is the calcium dialuminate or $CaAl_4O_7$. This compound has received great interest due to its low thermal expansion coefficient, fundamental property in terms of the resistance to thermal shock [14-16]. At present, there is no available report on sintering of this compound by SPS in the literature. Numerous authors reported that reaction sintering of $CaAl_4O_7$ from mixtures of pure chemical reactants such as $CaCO_3$ and Al_2O_3 by conventional heating is difficult and therefore, multiple stages of sintering are needed to obtain an acceptable degree of densification [15, 17-18]. For that, prior to sintering the $CaAl_4O_7$, three successive stages involving calcination at 1200, 1300 and 1450 °C followed by an intensive treatment of ball milling/ mixing and pressing at every stage must be applied [15]. However, the presence of residual calcium monoaluminate $CaAl_2O_4$ has been even detected.

In this work, the effect of two sintering techniques

*Corresponding author:
Tel : +011-54-2214840167
Fax: +011-54-221-4710075
E-mail: yesibruni@hotmail.com

(SPS and conventional sintering CS) on the crystalline phase composition, densification, microstructure and Vickers hardness of ZrO_2 - $CaAl_4O_7$ composites was evaluated. The composites were obtained using mixtures of two commercially available m- ZrO_2 powders (having different particle size distributions) and high alumina cement containing $CaAl_2O_4$ and $CaAl_4O_7$. Furthermore, the progress of stabilization of ZrO_2 with calcium which is the main reaction in these composites was evaluated by XRD.

Experimental

Materials and methods

The ZrO_2 - $CaAl_4O_7$ composites were prepared from mixtures of commercial powders of monoclinic zirconia (m- ZrO_2) and high alumina cement (HAC). Two commercial high purity m- ZrO_2 powders of different grain sizes were used: Zirconia (Saint-Gobain-ZirPro, China) with a mean particle size $d_{50} = 0.44 \mu m$ and ZrO_2 (Anedra, Research AG S.A., Germany) with a mean particle size $d_{50} = 8 \mu m$. The high alumina cement used of commercial grade (Secar 71, Kerneos, France) is commonly used in the refractory industry and mainly contains 68 wt% of Al_2O_3 and 30 wt% of CaO. In terms of the mineralogical composition of the Secar 71 determined by XRD, $CaAl_2O_4$ (CA) was the main phase (major active phase of refractory cements), $CaAl_4O_7$ (CA_2) was secondary phase and low amount of α - Al_2O_3 was detected. This cement has a wide range of particle size distribution, containing particles of variable size between 1 and $63 \mu m$, with $d_{50} = 13 \mu m$ [19].

From these starting materials (m- ZrO_2 and high alumina cement), different chemical compositions were prepared varying the m- ZrO_2 to HAC weight ratio to obtain between 5 and 50 mol% CaO in ZrO_2 . The green disks were shaped by uniaxial pressing (100 MPa) of the various powder mixtures. Thus, two series of composites were produced using ZrO_2 powders of different mean particle sizes. The composites prepared from ZrO_2 with $d_{50} = 8 \mu m$ and HAC are referred in this study as "ZC" and the other series prepared from ZrO_2 with $d_{50} = 0.44 \mu m$ are indicated as "ZCF".

Sintering and characterization of composites

Green compacts were sintered by two different techniques: one of them was the conventional sintering (CS) route in an electric furnace and the other was the spark plasma sintering technique (SPS).

For CS disks (30 mm of diameter, 5 mm of height) were pressed and subsequently sintered in air using a Thermolyne furnace at a heating rate of $5 \text{ }^\circ\text{C}/\text{min}$ up to different temperatures between 1200-1400 $^\circ\text{C}$ for two hours and then cooled to room temperature at $5 \text{ }^\circ\text{C}/\text{min}$. The Spark Plasma Sintering was performed using an SPS machine (SPS-1050, Sumitomo, Kawasaki, Japan).

The powders were placed in a graphite die with an inside diameter of 10 mm. The temperature was measured using an optical pyrometer focused on the die surface. Graphite filter was used to reduce the heat loss by radiation. The powder was heated from room temperature to 700 $^\circ\text{C}$ in 10 min., and subsequently to the sintering temperature (1200, 1300 and 1400 $^\circ\text{C}$). The heating rate was $300 \text{ }^\circ\text{C}/\text{min}$. The dwelling time was 10 min. and the applied pressure was 100 MPa.

The crystalline phases present in each composite were determined by X-ray diffraction (XRD) using a Philips model PW 3020 diffractometer with Cu-K α radiation and Ni filter in the region of $2\theta = 5$ -80 $^\circ$. The relative proportion of m- ZrO_2 phase was determined quantitatively using the XRD diagrams by the method of Garvie and Nicholson [20] for mixtures of stabilized zirconia and monoclinic phase.

The microstructure was analyzed by scanning electron microscopy (SEM-EDX). The apparent density was obtained by Hg immersion method. The relative density RD was calculated for each composite as the ratio between apparent density and the theoretical density, and then, the porosity was calculated as $P = 1 - RD$.

The hardness of the composites was evaluated on polished surfaces by Vicker's indentation technique (Buehler durometer, dentamet 1100, Serie Test Macro Vickers) according to ASTM C-1327 [21] with a load of 1 Kgf during 15 s for each material. The hardness reported represents the average value of ten indentations.

Results and Discussion

ZCF composites produced from fine m- ZrO_2 and HAC

Crystalline phase content and stabilization reaction of ZrO_2

The crystalline phases present in composites after sintering originated from two reactions: ZrO_2 stabilization with calcia and $CaAl_4O_7$ (CA_2) formation, occurring between m- ZrO_2 and HAC as starting materials.

Fig. 1 and 2 show the XRD patterns of the ZCF composites (fine zirconia) with 5, 15 and 30 mol% CaO in ZrO_2 sintered by SPS and SC at 1400 $^\circ\text{C}$ respectively. In general the amount of $CaAl_4O_7$ (phase originated from high alumina cement, HAC) and c- ZrO_2 (produced by the solid state reaction between CaO and m- ZrO_2) both increased with increasing of HAC content of composites while the content of m- ZrO_2 decreased due to its transformation as cubic phase. The c- ZrO_2 formation constituted the main reaction of this system.

It was not possible to detect the presence either of $CaAl_2O_4$ (CA) or free α - Al_2O_3 originated from the HAC addition, indicating that these phases have been completely reacted. The $CaAl_2O_4$ reacts with alumina between 1000 and 1200 $^\circ\text{C}$ to give $CaAl_4O_7$ which explains the absence of the $CaAl_2O_4$ phase [22].

The amount of $CaAl_4O_7$ and c- ZrO_2 increased both

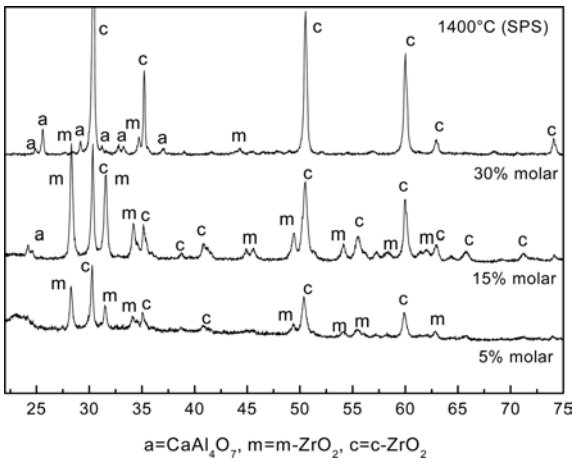


Fig. 1. XRD patterns of composites sintered by SPS at 1400 °C.

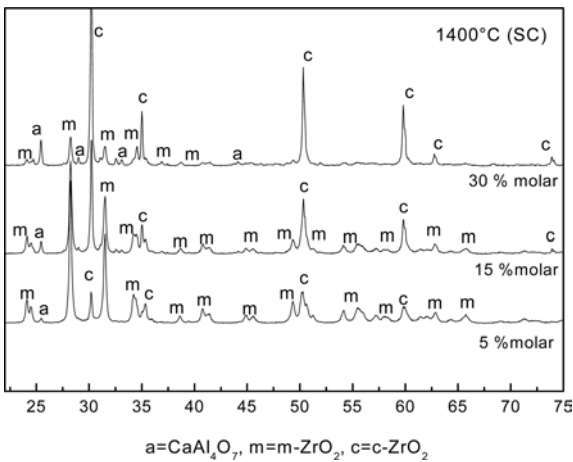


Fig. 2. XRD patterns of composites sintered by SC at 1400 °C.

with increasing cement content from 5 to 30 mol% CaO in ZrO₂. The composites with 5 and 15 mol% CaO in ZrO₂ in general consisted of a mixture of m-ZrO₂ and c-ZrO₂ (Ca_{0.15}Zr_{0.85}O_{1.85}) with a small amount of CA₂ (CaAl₄O₇) due to small content of HAC present in the starting compositions. The composites with 30 mol% consisted of a mixture of c-ZrO₂ and CA₂ with small amount of m-ZrO₂. In these composites the decrease in m-ZrO₂ content was observed according to the transformation as c-ZrO₂.

The XRD results of ZrO₂-HAC mixtures (with the same compositions previously analyzed) sintered at temperatures lower than 1400 °C revealed the presence of the same main phases (data not shown).

The main difference between CS and SPS composites was related to c-ZrO₂ formation as is present in Fig. 3 that shows the variation of m-ZrO₂ and c-ZrO₂ (cubic phase, Ca_{0.15}Zr_{0.85}O_{1.85}) with CaO content for the ZCF composites (determined by the Garvie and Nichosson method) produced by SPS and CS at 1300 and 1400 °C.

Generally c-ZrO₂ content increased with increasing of CaO content (as previously discussed) and with increasing of the sintering temperature, due to the advance of the reaction involved (that depends on diffusional mechanisms). Therefore the content of m-ZrO₂ decreased under the above conditions according to the transformation as c-ZrO₂. In fact the m-ZrO₂ amount abruptly decreased from 80 to <0.5 vol% with increasing HAC content from 5 to 50 mol% CaO as showed in Fig. 3a.

In composites with 5 mol% (with minor content of HAC) obtained by CS the small amount of CaO determined the lowest c-ZrO₂ formation and therefore the effect of sintering temperature was negligible. In these composites the content of cubic phase was ranged between 5 and 10 vol% whereas in composites 5 mol% obtained by SPS the content of this phase was higher and constituted nearly 28 vol% at 1400 °C.

The high efficiency of SPS technique on the activation of diffusion processes was remarkable for composites with 30 mol% CaO in ZrO₂. In these composites with high HAC content, the proportion of c-ZrO₂ significantly increased to a maximum of 45 vol% at 1300 and 1400 °C whereas the maximum content of CS composites attained close to 30 vol% at 1400 °C. In composites obtained by SPS and CS with 50 mol% the content of c-ZrO₂ decreasing to 25 vol%, in both cases the reduction to (<0.5 vol%) was due to the low content of m-ZrO₂ in the starting composition.

The XRD results obtained indicated that the type of sintering technique was an important factor influencing the c-ZrO₂ formation. The marked progress in the stabilization reaction of c-ZrO₂ by SPS it is probably

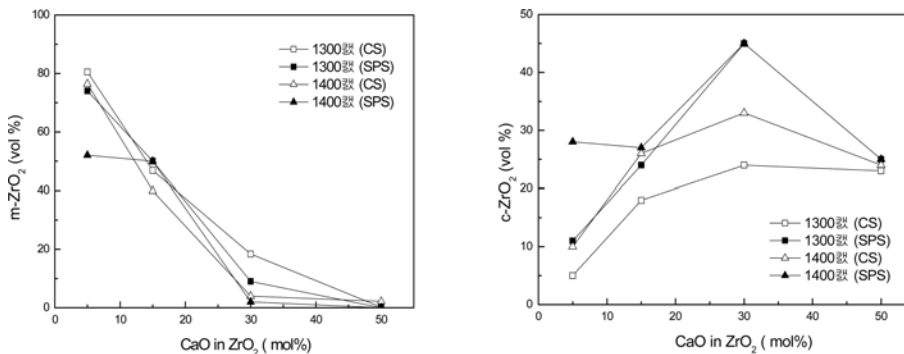


Fig. 3. (a) m-ZrO₂ and (b) c-ZrO₂ contents of ZCF composites sintered by SPS and CS at 1300 and 1400 °C.

due to the combination of several effects operating during SPS (electrical, thermal -high heating rates and high pressure applied). As will be discussed, this reaction in the present system occurred simultaneously with densification of the ceramics [23]. Further SPS can efficiently enhanced the diffusion processes involved, even in the presence of low CaO concentration which is the limiting factor to the progress of reaction for CS. The sintering temperature was the main parameter to accelerate the c - ZrO_2 reaction in composites obtained by CS.

Generally, SPS highly activated the mass diffusion processes involved in the densification and reaction processes due to the presence of the electric field and the high temperature gradient [24].

Densification

Fig. 4 shows the relative density of the different ZCF composites obtained by CS and SPS between 1200 and 1400 °C.

As expected, the densification degree of composites produced by SPS was significantly higher compared with that of composites obtained by CS. In general, SPS enhanced densification and therefore the composites attained high relative density (> 0.95) which indicated a final stage of sintering, independently of sintering temperature and composition. This result demonstrated the optimum densification degree obtained by SPS even at relatively lower temperatures which is one of the major advantages previously found for SPS technique including short sintering times as well as denser microstructures with a minimum in grain growth. The cited effects have been verified for sintered alumina powders and commercial nanometric ZrO_2 powders [25-29].

On the other hand, densification degree of composites produced by CS varied significantly between 0.59 and 0.9 depending on the composition and thermal treatment. Moreover, apparent density of these composites decreased with increasing CaO content for a constant sintering temperature. The high cement content of the starting composition led to an increase in the amount of $CaAl_4O_7$ which is the phase with lower density (2.91 g/cm^3) in relation to m - ZrO_2 (5.82 g/cm^3) and c - ZrO_2 (5.55 g/cm^3) [5]. Therefore, samples with 50 mol% CaO having 70 vol% of $CaAl_4O_7$ exhibited low relative density ranging from 0.62 to 0.73 after sintering at 1200 to 1400 °C. Contrarily, densification of these composites considerably increased by SPS reaching the relative density up to 0.97 for the range of temperatures analyzed. This is mainly associated with the electrical, thermal effects during SPS as well as the relative high pressure applied which also promoted disintegration of agglomerates present in the starting powder composition (i.e. $CaAl_4O_7$) as was found in previous studies [29-34].

Meanwhile, the composites with 5 mol% CaO produced by both SPS and CS at 1400 °C attained the

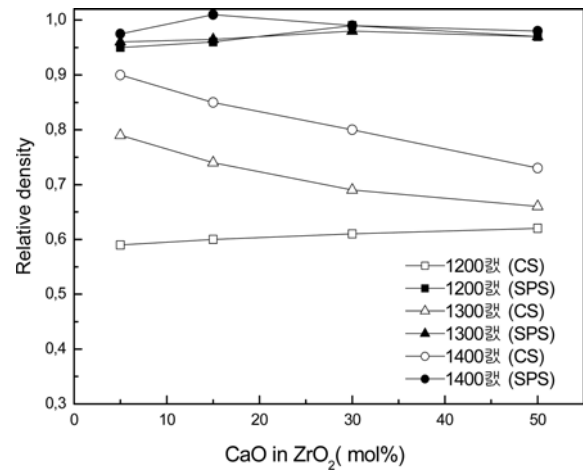


Fig. 4. Relative density of different ZCF composites produced by SPS and CS at 1200 -1400 °C.

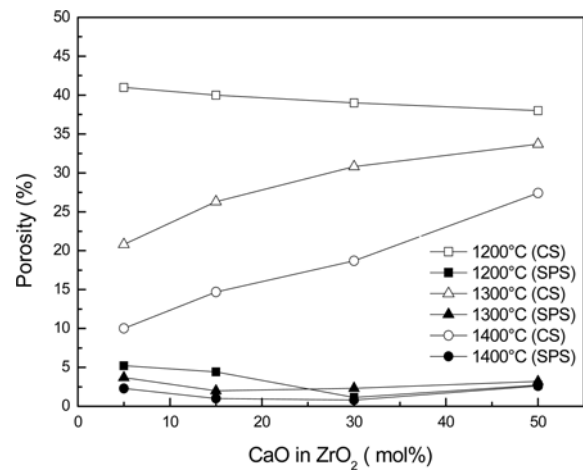


Fig. 5. Porosity of different ZCF composites sintered by SPS and CS at 1200-1400 °C.

highest relative densities (0.97 and 0.9, respectively) due to the combined effect of the composition and heat treatment effectiveness. In these composites, fine ZrO_2 was the major phase (80 vol%) whose effective sintering by CS usually occurs at 1450-1500 °C [35]. Moreover the difference in densification between composites using SPS and CS resulted more significant at 1200 °C, compared with that at 1300-1400 °C. At 1200 °C, the composite produced by CS exhibited the relative density of 0.6 indicating an incipient degree of sintering. Whereas, densities of composites processed by SPS at 1200 °C varied between 0.95 and 0.99 due to the optimum sintering as a result of the high effectiveness of SPS. Olevsky (2009) showed that high heating rates, which are characteristics of SPS process, produce a great activation of matter diffusion transport mechanism (grain boundary diffusion) and reduce the time of permanence at low sintering temperatures at which the surface diffusion mechanism dominates [25]. Wu and Brook (1984) previously investigated the densification mechanisms during sintering of CaO stabilized ZrO_2 by hot pressing and suggested that

densification was controlled by the interstitial lattice cation diffusion [23]. Bernard and Grizard (2007) investigated the possible mechanisms controlling densification for 3 mol% yttria stabilized ZrO_2 , in a form of commercial granulated powder when SPS was applied. These authors proposed that at intermediate macroscopic compaction stresses (pressure applied of 100 MPa and heating rates of 500 °C/min) and moderate temperatures (950 to 1050 °C) the densification by SPS proceeds by grain boundary sliding accommodated by an in series inter-diffusion: interface-reaction/lattice diffusion of Zr^{4+} and/ or Y^{+3} cations, mechanism controlled by the interface-reaction step [24].

Fig. 5 shows the porosity of the different composites sintered at 1300 and 1400 °C. The composites obtained by SPS showed low porosities < 4% without any appreciable effect of composition and heat treatment. SPS enhanced densification regarding to that of samples subjected to CS, leading to a marked difference in porosity between CS and SPS composites.

For CS, composition and sintering temperature were the main influencing factors to reduce porosity which is consistent with the densification behavior of such composites. Porosity reduced with decreasing HAC addition (i.e. low $CaAl_4O_7$ content in the sintered sample) and with increasing sintering temperature. Moreover, high porosity about 40% was obtained by CS at 1200 °C for all composites due to incipient degree of sintering, but porosity reduced to 21 and 11%

for 1300 and 1400 °C respectively, according to the compositional effect.

Microstructure

Fig. 6a and b show the SEM microstructure of the ZCF composites with 15 mol% CaO sintered at 1200 °C for CS and SPS, respectively. Both samples exhibited similar microstructures which consisted of ZrO_2 matrix (detected by EDX as white grains) containing dispersed $CaAl_4O_7$ agglomerates (dark gray grains) with different sizes. However, a significant difference in densification of the matrix was observed between composites subjected to CS and SPS. Fig. 6a clearly shows the porous ZrO_2 matrix of the composite processed via CS, the small interconnection between particles confirmed the incipient degree of sintering at 1200 °C.

Contrarily, SPS originated a dense ZrO_2 matrix at 1200 °C which evidenced the greater effectiveness of this sintering technique which promoted the formation of large necking area between particles and led to an enhanced densification.

Fig. 7a and b show the SEM microstructure of the composite with 30 mol% CaO sintered at 1300 °C by CS and SPS, respectively. In both composites, the high $CaAl_4O_7$ content caused a remarkable change in the microstructure configuration depending on the sintering technique. The composite processed by SPS exhibited a dense matrix of c- ZrO_2 containing dispersed coarse

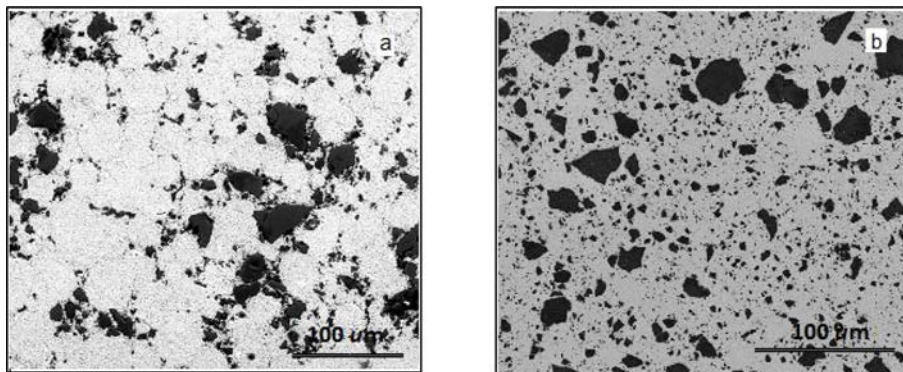


Fig. 6. SEM micrographs of ZCF composites with 15 mol% CaO sintered at 1200 °C by (a) CS and (b) SPS.

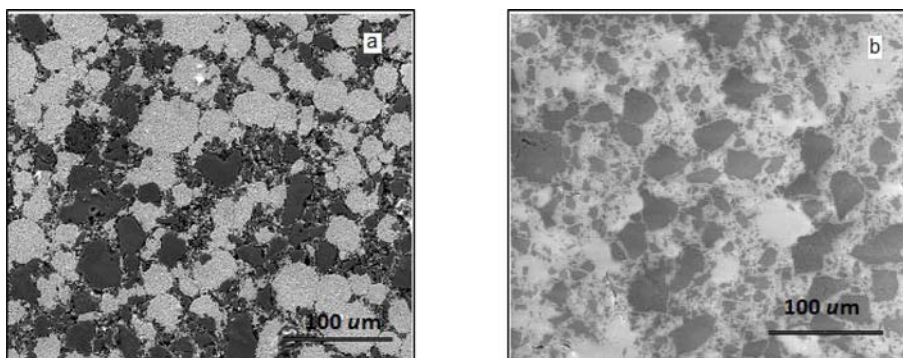


Fig. 7. SEM micrographs of ZCF composites with 30 mol% CaO sintered at 1300 °C by (a) CS and (b) SPS.

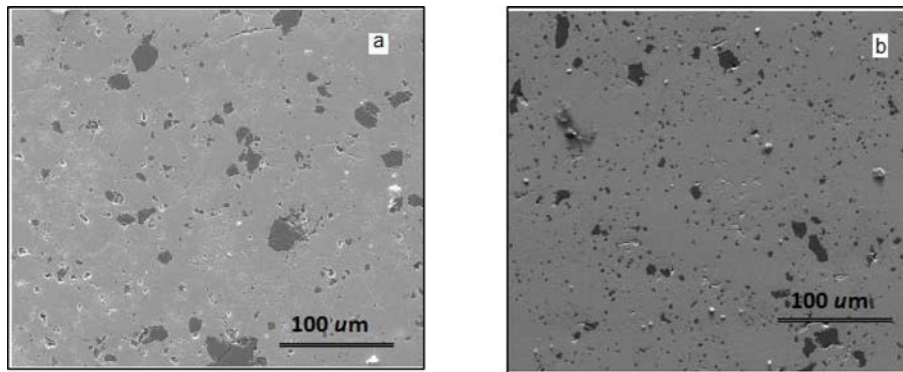


Fig. 8. SEM micrographs of ZCF composites with 5 mol% CaO sintered by (a) CS and (b) SPS at 1400 °C.

$CaAl_4O_7$ agglomerates, while the composite produced via CS showed a porous microstructure consisting of interconnected agglomerates of zirconia grains (monoclinic and cubic phases) and coarse $CaAl_4O_7$ grains. The intergranular porosity and the low formation of necking area between ZrO_2 particles evidenced the low degree sintering of this composite.

Fig. 8a and b show the microstructure examined by SEM of the composites with 5 mol% CaO in ZrO_2 produced via SC and SPS at 1400 °C. Efficient sintering resulted at 1400 °C regardless of the technique applied, but SPS led to highly dense composites.

Moreover, some microcracking appeared in the ZrO_2 matrix of composites subjected to CS whereas it can not be detected in composites obtained by SPS. This is attributed to the rapid cooling from the sintering temperature in SPS which probably prevented the ZrO_2 phase transformation leading to microcracking.

Hardness

Table 1 shows the Vickers hardness of ZrO_2 - $CaAl_4O_7$ composites produced by CS and SPS at 1300, and 1400 °C. The hardness of composites processed CS at 1200 °C can not be evaluated due to the excessive porosity. This property showed a strong variation with sintering technique employed since hardness mainly depends on the densification degree. The ZrO_2 - $CaAl_4O_7$ composite processed by SPS exhibited the maximum

hardness (~ 10 GPa) even at 1200 °C showing the high effectiveness of SPS to enhance densification at lower sintering temperatures. The SPS significantly improved densification and hence hardness due to rapid heating rates during sintering which inhibited the mass transport by surface diffusion mechanism and additionally promoted both volume and grain boundaries diffusion mechanisms. In general, SPS accelerates densification even at low temperatures while the grain growth is retained and consequently, enhancement in mechanical properties results. Many authors pointed out the great importance of electric energy discharge in accelerating densification processes [36-39].

Moreover, hardness of different ZrO_2 - $CaAl_4O_7$ composites (Table 1) was consistent with values previously determined for Ca-PSZ ceramics (8 mol% CaO) and Ca-FSZ (16 mol% CaO) obtained by microwave sintering at 1585 °C for 1 h. These ceramics reached relative density of 0.9 and Vickers hardness was between 8 and 10 GPa [10]. Thus, ZrO_2 - $CaAl_4O_7$ composites obtained by SPS exhibited acceptable hardness in terms of potential applications as an engineering ceramics.

Similarly, hardness of ZrO_2 - $CaAl_4O_7$ composites conventionally sintered increased with reducing porosity. Also, hardness depended on CaO content and thus, a decrease in hardness was determined with increasing CaO content (i.e. high $CaAl_4O_7$ content in the sintered sample). Therefore, composites with 5 and 15 mol% CaO produced by CS at 1400 °C reached similar hardness of 6 GPa due to relatively low porosity and small amount of $CaAl_4O_7$, while hardness reduced to 4 GPa for porous composite with 30 mol% of CaO.

Certainly, the lower hardness corresponded to composites with 50 mol% CaO which mainly consisted of $CaAl_4O_7$ (70 vol%). The $CaAl_4O_7$ content did not influence the hardness of ceramics obtained by SPS due to the high densification degree for all compositions studied.

Densification and c- ZrO_2 formation for ZC composites produced from coarse m- ZrO_2 by SPS and CS.

The effect of the coarse particle size of starting m-

Table 1. Vickers Hardness of ZrO_2 - $CaAl_4O_7$ composites (ZCF) produced via different techniques: conventional (CS) and spark plasma sintering (SPS).

Composition CaO in ZrO_2 (mol %)	Vickers Hardness (GPa)				
	1200 °C		1300 °C		1400 °C
	SPS	CS	SPS	CS	SPS
5	8.7 ± 0.7	4 ± 0.2	9 ± 0.3	6 ± 0.3	9 ± 0.4
15	8.7 ± 0.4	3 ± 0.3	9 ± 0.3	6 ± 0.5	10 ± 0.6
30	9.7 ± 0.7	n.d.	9 ± 0.6	4 ± 0.3	9 ± 0.4
50	9.2 ± 0.5	n.d.	9 ± 0.4	n.d.	9.5 ± 0.5

(n.d.: not determined due to excessive porosity).

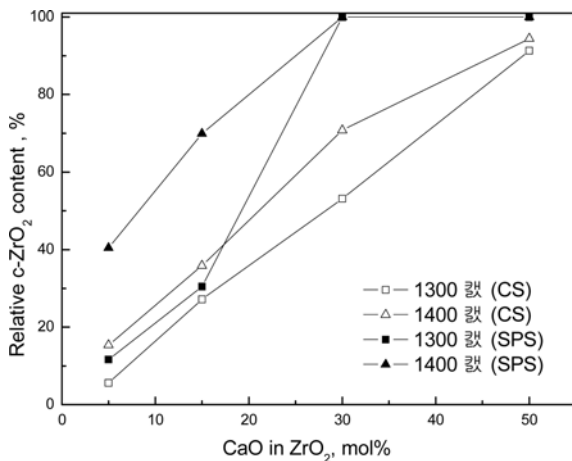


Fig. 9. Effect of composition and sintering technique on relative c-ZrO₂ content for ZC composites sintered at 1300 and 1400 °C.

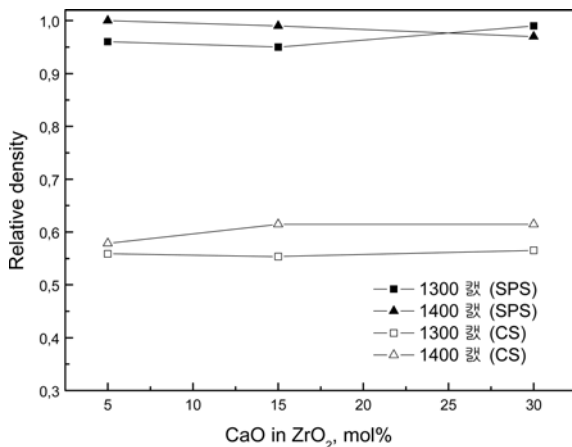


Fig. 10. Effect of sintering technique on the densification degree of ZC composites sintered at 1300 and 1400 °C.

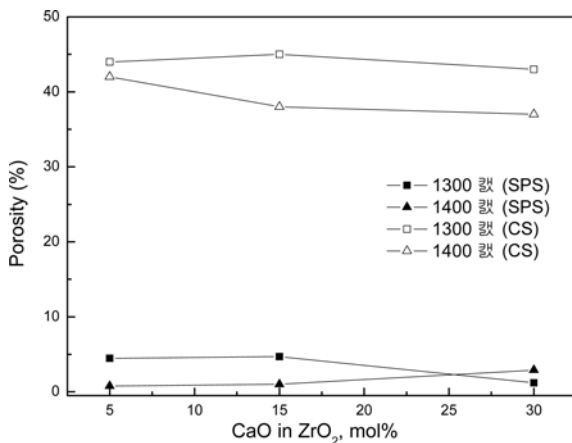


Fig. 11. Effect of sintering technique on the porosity of ZC composites sintered at 1300 and 1400 °C.

ZrO₂ powder on reaction and densification of ZrO₂-CaAl₄O₇ composites processed by SPS and with the use of CS were examined. Fig. 9 shows the effect of composition and sintering technique on c-ZrO₂ phase formation between 1300 and 1400 °C. In terms of the reaction of stabilization ZrO₂ with CaO of ZC samples,

similar dependence was observed compared with ZCF composites produced from submicrometer sized m-ZrO₂. The relative c-ZrO₂ proportion (with respect to total ZrO₂) was slightly higher for composites produced by SPS regarding to those processed by CS. Except for composites with 50 mol% CaO in which the high CaO content led to complete ZrO₂ stabilization regardless of the technique used.

Fig. 10 shows the relative density of ZC composites processed by SPS and CS at 1300 and 1400 °C. Highly dense ZC composites were obtained by SPS (>0.95) (Fig. 4). Comparatively, ZC composites conventionally sintered attained lower relative densities between 0.55 and 0.62 at the same sintering temperatures indicating an initial stage of sintering. SPS originated dense ZC composites with low porosities (1-5%) while porous composites were developed by CS with porosities between 38 and 44%. Thus, SPS represented considerable improvement in densification for both ZC and ZCF composites but the most important changes in densification by SPS occurred when ceramics were produced from m-ZrO₂ mixtures with coarse particle size as starting powder.

Conclusions

Ca stabilized ZrO₂-CaAl₄O₇ composites were sintered using two different techniques: via conventional sintering (CS) and Spark Plasma (SPS) between 1200 and 1400 °C. ZrO₂ could be stabilized in a cubic phase (Ca_{0.15}Zr_{0.85}O_{1.85}) even with 5 mol% CaO addition (i.e. small amount of HAC as a source of CaO) by an in situ reaction between m-ZrO₂ and HAC. The c-ZrO₂ formation, main reaction in the system, was accelerated by SPS due to the matter transport involved in the reaction was strongly promoted. The formation of c-ZrO₂ derived a potential use of the composite as engineering ceramics.

Therefore SPS promoted a marked improvement in densification for ZC and ZCF composites, produced using coarse and fine m-ZrO₂ respectively, attaining relative density higher than 0.95 even at 1200 °C, which is a temperature very inefficient for conventional sintering. In composites with small content of CaAl₄O₇ sintered at 1400 °C exhibited improvements in final density for both sintering techniques. In fact the advantage of SPS technique was mainly evidenced by the high densification of composites with high CaAl₄O₇ content.

The highest density was 0.99 for SPS at 1400 °C for 10 min while density was 0.9 for CS at 1400 °C for 2 h, this evidenced that sintering time significantly reduced by SPS. Nevertheless, processing parameters like m-ZrO₂ particle size, and composition weakly influenced the degree of densification using SPS. In general, the Vickers hardness of dense ZrO₂-CaAl₄O₇ composites sintered by SPS reached 9 GPa.

Dense ZrO₂-CaAl₄O₇ ceramics were produced by

conventional pressureless sintering CS with the use of fine-sized m - ZrO_2 as a reactant (ZCF composites) and thus, attained hardness of 6 GPa. The increase in particle size of m - ZrO_2 to the micrometer range significantly reduced the sinterability of the powder mixtures, and the particle size reduction played an important role in the densification of ZrO_2 - $CaAl_4O_7$ composites by CS.

References

1. M. Omori, Sintering, consolidation, reaction and crystal growth by the spark plasma system (SPS), *Mat. Sci. Eng.*; 287 (2000) 183-188.
2. R. Orru, R. Licheri, A. M. Locci, A. Cincotti, G. Cao, Consolidation/synthesis of materials by electric current activated/assisted sintering, *Mat. Sci. Eng.*; 63 (2009) 127-287.
3. S. Grasso, Y. Sakka, G. Maizza, Electric Current Activated/ Assisted Sintering (ECAS): A Review of Patents 1906-2008, *Sci. Technol. Adv. Mater.* 10 (2009).
4. Y.L. Bruni, L.B. Garrido, E.F. Aglietti, Reaction and phases from monoclinic zirconia and calcium aluminate cement at high temperatures *Ceram. Int.*; 38 (2012) 4237-4244.
5. R. Muccillo, R.C. Buissa Netto, E.N.S. Muccillo, Synthesis and characterization of calcia fully stabilized zirconia solid electrolytes, *Mater. Lett.*; 49 (2001) 197-201.
6. H.H. Zender, H. Leistner, H. Searle, ZrO_2 materials for application in the ceramic industry, *Ceram. Int.*; 39 (1990) 33-38.
7. S. Nath, N. Sinha, B. Basu, Microstructure, mechanical and tribological properties of microwave sintered calcia-doped zirconia for biomedical applications, *Ceram. Int.*; 34 (2008) 1509-1520.
8. E. Mustafá, Ca-PSZ prepared via polymeric sol-gel route, *Ceram. Int.*; 26 (2000) 215-220.
9. J. Carretero, M.A. Sainz, S. Serena, A. Caballero, Obtención de circonas estabilizadas (Ca, Mg-PSZ) nanocristalinas a partir de mezclas de dolomita y circonia monoclinica mediante molienda de alta energía, *Bol. Soc. Esp. Ceram. Vidr.*; 42 (2003) 303-310.
10. V. Silva, L. F. Soares, D. R. Zacarias, Synthesis and characterization of calcia partially stabilized zirconia-hydroxyapatite powders prepared by co-precipitation method, *Ceram. Int.*; 27 (2001) 615-620.
11. K. Rajeswari, M. Buchi Suresh, U.S. Hareesh, Y. Srinivasa Rao, D. Das, R. Johnson, Studies on ionic conductivity of stabilized zirconia ceramics (8YSZ) densified through conventional and non-conventional sintering methodologies, *Ceram. Int.*; 37 (2011) 3557-3564.
12. X. Miao, Y. Chen, H. Guo, K. Aik Khor, Spark plasma sintered hydroxyapatite-ytria stabilized zirconia composites, *Ceram. Int.*; 30 (2004) 1793-1796.
13. Q. Li, Y.F. Zhang, X.F. Ma, J. Meng, X.Q. Cao, High-pressure sintered yttria stabilized zirconia ceramics, *Ceram. Int.*; 35 (2009) 453-456.
14. Y. Suzuki, T. Ohji, Anisotropic thermal expansion of calcium dialuminate ($CaAl_4O_7$) simulated by molecular dynamics, *Ceram. Int.*; 30 (2004) 57-61.
15. S. Jonas, F. Nadachowski, D. Szwagierczak, Low thermal expansion refractory composites based on $CaAl_4O_7$, *Ceram. Int.*; 25 (1999) 77-84.
16. S. Jonas, F. Nadachowski, D. Szwagierczak, G. Wójcik, Thermal expansion of $CaAl_4O_7$ -based refractory compositions containing MgO and CaO additions, *J. Eur. Ceram. Soc.*; 26 (2006) 2273-2278.
17. J.D. Kenneth, T. Jadambaa, T. Mack Kenzie, J. Banzar, N. Budjav, M. Olziiburen, E. Smith, P. Angerer, Effect of mechanochemical treatment on the synthesis of calcium dialuminate, *J. Europ. Mat. Chem.*; 10 (2000) 1019-1023.
18. B. Singh, A.J. Majumdar, The hydration of calcium dialuminate and its mixtures containing slag, *Cement and Concrete Res.*; 22 (1992) 1019-1026.
19. M.A.L. Bralio, G.G. Morbioli, D.H. Milanez, V.C. Pandolfelli, Calcium aluminate cement source evaluation for Al_2O_3 -MgO refractory castables, *Ceram. Int.*; 37 (2011) 215-221.
20. R. Garvie, P.S. Nicholson, Phase Analysis in Zirconia Systems, *J. Am. Ceram. Soc.*; 55 (1972) 303-305.
21. ASTM C1327, Standard Test Method for Vickers Indentation Hardness of Advanced Ceramics (2008).
22. W.E. Lee, W. Vieira, S. Zhang, K.G. Arari, H. Sarpoolaky, C. Parr, Castable refractory concretes, *Inter. Mater. Rev.*; 46 (2001) 145-167.
23. S.X. Wu, R.J. Brook, Kinetics of densification in stabilized zirconia, *Solid States Ionics* 14 (1984) 123-130.
24. G. Bernard-Granger, C. Guizard, Apparent activation energy for the densification of a commercially available granulated zirconia powder, *J. Am. Ceram. Soc.* 90 (2007) 1246-1250.
25. E. Olevsky, Impact of thermal diffusion on densification during SPS, *J. Am. Ceram. Soc.* 92 (2009) 122-132.
26. Y. Zhou, K. Hirao, Y. Yamauchi, S. Kansaki, Effects of heating rate and particle size on pulse electric current sintering of alumina, *Scripta Mater.* 48 (2003) 1631-1636.
27. M. Demuyneck, J.P. Erauw, O. Van der Biest, F. Delannay, F. Cambier, Densification of alumina by SPS and HP: A comparative study, *J. Europ. Soc.* 32 (2012) 1957-1964.
28. L. Liu, Z. Hou, B. Zhang, F. Ye, Z. Zhang, Y. Zhou, A new heating route of spark plasma sintering and its effect on alumina ceramic densification, *Mat. Sci. Eng.* 559 (2013) 462-466.
29. Z. Shen, M. Johnsson, Z. Zhao, M. Nygren, Spark Plasma Sintering of Alumina, *J. Am. Ceram. Soc.* 85 (2002) 1921-1927.
30. S. W. Wang, L. D. Chen, T. Hirai, Densification of Al_2O_3 powder using spark plasma sintering, *J. Mater. Res.* 15 (2000) 982-987.
31. Y. Zhou, K. Hirao, Y. Yamauchi, S. Kansaki, Densification and grain growth in pulse electric current sintering of alumina, *J. Eur. Ceram. Soc.* 27 (2007) 3331-3337.
32. Z. A. Munir, U. Anselmi-Tamburini, M. Ohyanagi, The effect of electric field and pressure on the synthesis and consolidation of materials: A review of the spark plasma sintering method, *J. Mat. Sci.* 41 (2006) 763-777.
33. Z.A. Munir, D.V. Quach, Electric Current Activation of Sintering: A Review of the Pulsed Electric Current Sintering Process, *J. Am. Ceram. Soc.* 94 (2011) 1-19.
34. D.V. Quach, H. Avila-Paredes, S. Kim, M. Martin, Z.A. Munir, Pressure effects and grain growth kinetics in the consolidation of nanostructured fully stabilized zirconia by pulsed electric current sintering, *Acta Mater.* 58 (2010) 5022-5030.
35. D. Michel, F. Faudot, E. Gaffet, L. Mazerolles, Stabilized zirconias prepared by mechanical alloying, *J. Am. Ceram. Soc.* 76 (1993) 2884-2888.
36. U. Anselmi-Tamburini, S. Gennari, J.E. Garay, Z.A. Munir, Fundamental investigations on the spark plasma sintering/synthesis process: II. Modeling of current and temperature distributions, *Mat. Sci. Eng.* 394 (2005) 139-148.

37. W. Chen, U. Anselmi-Tamburini, J.E. Garay, J.R. Groza, Z.A. Munir, Fundamental investigations on the spark plasma sintering/synthesis process: I. Effect of dc pulsing on reactivity, *Mat. Sci. Eng.* 394 (2005) 132-138.
38. R. S. Mishra, , A. K. Mukherjee, Electric pulse assisted rapid consolidation of ultrafine grained alumina matrix composites, *Mat. Sci. Eng.* 287 (2000) 178-182.
39. D. Tiwari, B. Basu, K. Biswas, Simulation of thermal and electrical field evolution during spark plasma sintering. *Ceram. Int.* 35 (2009) 699-708.